Inorganic Chemistry
Article

Redox Induced Reversible Structural Transformations of Dimeric and Polymeric Phenanthroline-Based Copper Chelates

Stefan Bernhard, Kazutake Takada, David Jenkins, and Héctor D. Abruña*

Department of Chemistry and Chemical Biology, Baker Laboratory, Cornell University, Ithaca, New York 14853-1301

The synthesis and characterization of copper complexes of the phenanthroline based bridging ligands, 9-methyl-2-(2-{4-[2-(9-methyl-1,10-phenanthrolin-2-yl)ethyl]phenyl}ethyl)-1,10-phenanthroline, **1**, and 1,12-bis(9-methyl-1,-10-phenanthroline-2-yl)dodecane, **2**, are presented. Whereas in the first case a discrete dimeric complex $[Cu_2(\mathbf{1})_2](BF_4)_2$ was formed, in the latter, a coordination polymer $[\mathbf{2}(Cu(\mathbf{2}))_n](BF_4)_n$ resulted. Both of these materials have been characterized by cyclic voltammetry (CV), the electrochemical quartz crystal microbalance (EQCM), and UV–vis spectroscopy and the results compared to those of the monomeric $[Cu(dmp)_2](BF_4)$ (dmp is 2,9-dimethyl-1,10-phenanthroline) species. Oxidation of the dimeric species results in its precipitation and reduction results in stripping of the deposited layer as ascertained from CV and EQCM measurements. The electrooxidation of the copper centers in the coordination polymer results in changes in the coordination which are fully reversible upon reduction. The dissociation/regeneration of the coordination polymer as a function of the redox state of the copper centers has been characterized by CV, EQCM, and UV–vis spectroelectrochemistry.

Introduction

Copper(I) complexes of 2,9-substituted 1,10-phenanthrolines have been and continue to be a primary area of interest in contemporary transition metal coordination chemistry. Initially numerous studies were geared toward their use as metal-selective analytical tools.[1] More recently there has been a renewed interest in the photochemical properties of copper-(I) bis-1,10-phenanthroline compounds as candidates for the development of photonic devices including sensors, photovoltaic devices, and switches.[2] The photochemical and electrochemical properties of copper(I) phenanthroline compounds have also been used to study their interaction with biological systems, in particular DNA intercalation and scission.[3] There have also been numerous studies of these types of complexes in relation to their biomimetic behavior.[4]

Moreover, the redox chemistry of copper phenanthrolines is of particular interest due to the fact that $[Cu(phen)_2]^{+/2+}$ undergoes a coordination change during redox processes, from a four-coordinate tetrahedral geometry (T-4) in the Cu(I) state (d^{10}) to a five-coordinate (or six-coordinate) state with a less clearly defined stereochemistry, upon oxidation to Cu(II). The ability to deliberately control the microstructure of a coordination polymer by using macroscopic principles, through dissociation/binding ligands from/to metal centers by the applied potential, could have numerous materials applications. With the goal of using this feature to design electrochemically driven molecular motors and machines, Sauvage and co-workers prepared unique rotaxane and catenane structures based on copper(I) complexes of 2,9-substituted 1,10-phenanthrolines.[5] One outstanding example is the electrochemially induced ring-gliding in copper complexed catenanes, where two interlocking rings containing a 2,2′:6′,2″-terpyridine and a 2,9-substituted phenanthroline unit are connected through a copper(I) metal center employing the two phenanthroline ligands. The use of this supramolecular structure made it possible to deliberately switch between coordination sites through oxidation and reduction of the metal center.[6]

* To whom correspondence should be addressed. E-mail: hda1@cornell.edu.

(1) Diehl, H.; Smith, G. F.; Shildt, A. A.; McBride, L. C. *The Copper Reagents, Cuproine, Neocuproine, Bathocuproine*, 2nd ed.; G. F. S. Publications: Powell, OH, 1972.
(2) (a) Baranoff, E.; Colin, J. P.; Furusho, Y.; Laemmel, A. C.; Sauvage, J. P. *Chem. Commun.* **2000**, 1935–1936. (b) Castellano, F. N.; Meyer G. J. *Prog. Inorg. Chem.* **1997**, *44*, 167–208. (c) Miller, M. T.; Karpishin T. B. *Sens. Actuators* **1999**, *61*, 222–224.
(3) McMillin, D. R.; McNett, K. M. *Chem. Rev.* **1998**, *98*, 1201–1209.
(4) Solomon, E. I.; Sundaram, U. M.; Machonkin, T. E. *Chem. Rev.* **1996**, *96*, 3–2605.

(5) Sauvage, J. P. *Acc. Chem. Res.* **1998**, *31*, 611–619.

An extension of the work on mononuclear copper(I) bis-phenanthroline compounds, in part stimulated by the structural elucidation of several mono-, di-, tri-, and tetranuclear copper-containing biomolecules,[7] is the preparation of polynuclear structures. This area was pioneered by Lehn with the preparation of dimeric copper complexes from 1,10-phenanthroline-containing bridging ligands.[8] Later, similar ligands were used to prepare grid-type, helical, double-helical, and cylindrical structures and their properties, especially the photochemical behavior, were studied thoroughly.[9]

As a consequence of the work pursued in the area of multinuclear coordination compounds, an interest in polymeric redox and photoactive copper based materials has emerged. In an attempt to engineer photovoltaic devices, the photochemical properties were combined with the unique electronic properties of conducting polymers. For example, pyrrol and oligothienyl moieties were connected to mononuclear bis-1,10-phenanthroline copper complexes and the spectroelectrochemical behavior of polymers obtained through electropolymerization with these precursors was studied.[10] Rehahn et al. synthesized a *p*-phenylene bridged copper(I) polymer based on 2,9-aryl-1,10-phenanthroline and studied metal exchange mechanisms with Ag(I) through NMR spectroscopy.[11]

With the intent of generating a polymeric system with reversible binding/unbinding based on electron transfer, we report on the synthesis and characterization (NMR, MS, UV−vis spectroscopy) of novel copper(I) complexes containing two 2,9-dimethyl-1,10-phenanthroline (dmp) moieties which are linked by either a *p*-xylene or an *n*-decane bridge (Figure 1). Whereas the *p*-xylene bridged ligand formed a dimeric structure, the less rigid decane bridged ligand produced polymers. Using electrochemical, electrochemical quartz crystal microbalance (EQCM), and spectroscopic (UV−vis) techniques, the difference in redox behavior of the two complexes was studied and their behavior compared to that of the monomeric [Cu(dmp)$_2$](BF$_4$).

Experimental Section

Materials and Techniques. Lithium diisopropylamide (2 M) was purchased from Aldrich Chemical Co. and used as received. Methylene chloride (B&J) was dried over 4 Å molecular seives
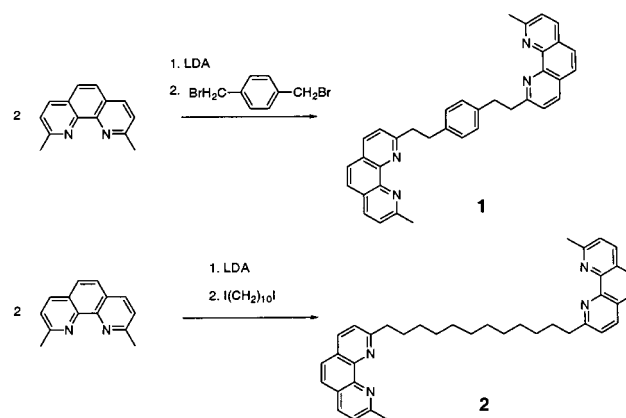
Figure 1. Synthetic pathways for the preparation of the two bridging ligands **1** and **2** through a 2-fold alkylation reaction of α,α′-dibromo-*p*-xylene or 1,10-diiododecane with 2,9-dimethyl-1,10-phenanthroline.

for 3 days. Tetra-*n*-butylammonium perchlorate (TBAP, GFS Chemicals) was recrystalized three times from ethyl acetate and dried under vacuum for 96 h. All other solvents were used without further purification. All other reagents were purchased from Aldrich and used as received. Column chromatography alumina was purchased from ICN Biomedicals GmbH.

^{1}H and ^{13}C NMR spectra were obtained on a Varian 200 (200 MHz) and Varian Nova 400 (400 MHz) spectrometers in dichloromethane-d_2 or chloroform-d_3. Coupling constants are given in hertz. Mass spectra were recorded at the Cornell mass spectrometry facility on a Micromass Quattro 1 triple quadrupole tandem mass spectrometer operated in electrospray ionization mode. UV−vis spectra were recorded using a Hewlett-Packard 8453 or a 8451A diode array spectrometer. For the spectrophotometric titration, 250 mL of a 40 μmol/L solution of **2** in dichloromethane was titrated with 10 μL increments of a 50 mM [Cu(CH$_3$CN)$_4$](PF$_6$) solution and the UV−vis spectra were measured in a 1 cm quartz cell. Elemental analysis was performed by Galbriath Laboratories, Inc., Knoxville, TN.

Electrochemical experiments were carried out with a BAS CV-27 potentiostat. Three compartment electrochemical cells (separated by medium porosity sintered glass disks) were employed. A platinum disk sealed in glass was used as the working electrode. Prior to use, the electrodes were polished with 1 μm diamond paste (Buehler) and rinsed with water and acetone. A coiled platinum wire was used as the counter electrode. All potentials are referenced to a Ag/AgCl electrode without regard for the liquid junction potential. For rotating disk electrode (RDE) experiments, a Pine Instruments analytical rotator and speed controller were utilized. The EQCM apparatus and instrumentation for resistance parameter measurements of the resonator have been previously described.[12]

Synthesis. (a) Ligand 1: C$_{36}$H$_{30}$N$_4$, 9-Methyl-2-(2-{4-[2-(9-methyl-1,10-phenanthrolin-2-yl)ethyl]phenyl}ethyl)-1,10-phenanthroline. Lithium diisopropyl amide (6.0 mmol, (3 mL, 2 M) in addition to a sufficient quantity to react with the water of hydration, which was indicated when the solution started turning blue (ca. 2.5 mL)) was added via syringe to a stirred solution of 2,9-dimethyl-1,10-phenanthroline (1.00 g, 4.8 mmol) in tetrahydrofuran (THF) at −40 °C under N$_2$. The deep blue solution was allowed to warm to −5 °C and kept at this temperature for 1 h. After cooling to −20 °C, α,α′-dibromo-*p*-xylene (0.50 g, 1.88 mmol) dissolved in THF was added via syringe. The reaction was allowed to continue

(6) Livoreil, A.; Dietrich-Buchecker, C. O.; Sauvage, J. P. *J. Am. Chem. Soc.* **1994**, *116*, 9399−9400.

(7) (a) Holm, R. H.; Kennepohl; P. Soloman, E. I. *Chem. Rev.* **1996**, *96*, 2239. (b) Soloman, E. I.; Sundaram, U. M.; Machonkin, T. E. *Chem. Rev.* **1996**, *96*, 2563. (c) Karlin, K. D.; Tyeklár, Z. *Bioinorganic Chemistry of Copper*; Chapman and Hall: New York, 1993.

(8) Youinou, M. T.; Ziessel, R.; Lehn, J. M. *Inorg. Chem.* **1991**, *30*, 2144−2148.

(9) (a) Baxter, P.; Lehn; J. M.; Decian, A.; Fischer, J. *Angew. Chem., Int. Ed. Engl.* **1993**, *32*, 69−72. (b) Kramer, R.; Lehn; J. M.; Decian, A.; Fischer, J. *Angew. Chem., Int. Ed. Engl.* **1993**, *32*, 703−706. (c) Baxter, P. N. W.; Hanan, G. S.; Lehn, J. M. *Chem. Commun.* **1996**, 2019−2020. (d) Slieman, H.; Baxter, P.; Lehn, J. M. Rissanen, K. *J. Chem. Soc., Chem. Commun.* **1995**, 715−716. (e) Marquis-Rigault A.; Dupont-Gervais, A.; Baxter P. N. W.; Van Dorsselaer, A.; Lehn, J. M. *Inorg. Chem.* **1996**, *35*, 2307−2310.

(10) (a) Vidal, P. L.; Divisia-Blohorn, B.; Bidan, G.; Hazemann, J. L.; Kern, J. M.; Sauvage, J. P. *Chem. Eur. J.* **2000**, *6*, 1663−1673. (b) Bidan, G.; Divisia-Blohorn, B.; Lapkowski, M.; Kern, J. M.; Sauvage, J. P. *J. Am. Chem. Soc.* **1992**, *114*, 5986−5994.

(11) Velten, U.; Rehahn, M. *Chem. Commun.* **1996**, 2639−2640

(12) Takada, K.; Díaz, D.; Abruña, H. D.; Cuadrado, I.; Casado, C.; Morán M.; Morán, Losada, J. *J. Am. Chem. Soc.* **1997**, *119*, 10763.

for 4 h, and the solution was left to reach room temperature. The reaction was quenched with 10% NH_4Cl (400 mL), and then the solution was extracted with CH_2Cl_2 (3 × 200 mL). The remaining reactant was removed with an extraction with aqueous HCl (3 × 100 mL, 0.1% HCl (v/v)). The organic phase was washed once with 5% $NaHCO_3$ solution and twice with water. The solvent was evaporated and the product was purified via column chromatography on alumina (neutral) using ether as eluent. Yield: 0.31 g (0.5 mmol, 32%) Anal. Calcd for $C_{36}H_{30}N_4 \cdot H_2O$: C, 80.57; H, 6.01; N, 10.44. Found: C, 80.58; H, 6.15; N, 9.68. ^1H NMR (CDCl$_3$): δ 8.14 (m, 4H), 7.71 (s, 4H), 7.51 (d, 4H, $J = 8$ Hz), 7.48 (s, 2H), 7.25 (s, 4H), 3.54 (t, 4H, $J = 6$ Hz), 3.25 (t, 4H, $J = 5$ Hz), 2.95 (s, 6H). ^{13}C NMR (CDCl$_3$): δ 162.24, 159.46, 145.51, 145.42, 139.44, 136.33, 136.30, 128.65, 127.24, 126.89, 125.64, 125.52, 123.50, 122.72, 41.20, 35.46, 26.07. HR-MS (ESI). Calcd for $C_{36}H_{31}N_4$ (M+H$^+$): 519.2549. Found: 519.2553.

(b) Ligand 2: $C_{38}H_{42}N_4$, 9-Methyl-2-[12-(9-methyl-1,10-phenanthrolin-2-yl)dodecyl]-1,10-phenanthroline. Lithium diisopropyl amide (24 mmol (12 mL, 2 M)), in addition to a sufficient quantity to react with the water of hydration, which was indicated when the solution turned blue) was added via syringe to a stirred solution of 2,9-dimethyl-1,10-phenanthroline (5.00 g, 24 mmol) in THF at −40 °C under N_2. The deep blue solution was allowed to warm to −5 °C and kept at this temperature for 1 h. After cooling to −20 °C 1,10-diiododecane (3.12 g, 7.9 mmol) dissolved in THF was added via syringe. The reaction was allowed to continue for 4 h. and the solution was left to reach room temperature. The mixture was quenched with 10% NH_4Cl (400 mL), and then the solution was extracted with CH_2Cl_2 (3 × 200 mL). The remaining reactant was removed with an extraction with aqueous HCl (9 × 200 mL, 0.5% HCl (v/v)). The product was recovered through an additional acidic extraction with HCl (4 × 200 mL, 5% HCl (v/v)). The acidic extract was neutralized with $NaHCO_3$, which caused the product to precipitate out of solution. It was filtered and then extracted with CH_2Cl_2 (3 × 300 mL). Yield: 2.5 g (4.5 mmol 57%) Anal. Calcd for $C_{38}H_{42}N_4$: C, 80.96; H, 7.69; N, 9.94. Found: C, 81.37; H, 7.70; N, 9.29.

^1H NMR (CDCl$_3$): δ 8.12 (d, 2H, $J = 9$ Hz), 8.09 (d, 2H, $J = 9$ Hz), 7.67 (s, 4H), 7.51 (d, 2H, $J = 9$ Hz), 7.46 (d, 2H, $J = 8$ Hz), 3.20 (t, 4H, $J = 8$ Hz), 2.93 (s, 6H), 1.88 (quintet, 4H, $J = 5$ Hz), 1.48 (quintet, 4H, $J = 6$ Hz), 1.30 (m, 12H). ^{13}C NMR (CDCl$_3$): δ 163.45, 159.33, 145.51, 145.29, 136.23, 127.05, 126.82, 125.48, 125.41, 123.40, 122.37, 39.69, 29.94, 29.88, 29.68, 29.64, 26.03. HR-MS (ESI). Calcd for $C_{38}H_{43}N_4$ (M + H$^+$): 555.3488. Found: 555.3497.

(c) [Cu$_2$(1)$_2$](BF$_4$)$_2$. The xylene-bridged ligand (1) (57 mg, 0.11 mmol) was dissolved in 20 mL of CH_2Cl_2 under N_2 gas and [Cu(CH$_3$CN)$_4$](BF$_4$) (35 mg, 0.11 mmol) dissolved in thoroughly degassed CH_3CN was added via syringe. The reaction was allowed to continue for 2 h, and the product was precipitated through the addition of acetonitrile and filtered. The product was purified via an ether diffusion crystallization. Anal. Calcd for $(C_{36}H_{30}N_4)_2Cu_2$-(BF$_4$)$_2$: C, 64.63; H, 4.52; N, 8.37. Found: C, 62.43; H, 4.66; N, 8.08. ^1H NMR (CD$_2$Cl$_2$, 400 MHz) δ 8.50 (2H, bs), 8.01 (2H, bs), 7.72 (2H, bs), 5.69 (2H, s), 2.92 (2H, m), 2.43 (5H, m). ESI-MS (m/z): 581 (100%, [M - 2BF$_4$]$^{2+}$).

(d) [2(Cu(2))$_n$](BF$_4$)$_n$. Under an atmosphere of nitrogen, the dodecane bridged ligand 2 (277 mg, 0.5 mmol) was dissolved in 20 mL of CH_2Cl_2. Subsequently, [Cu(CH$_3$CN)$_4$](BF$_4$) (157 mg, 0.5 mmol) dissolved in 20 mL of acetonitrile was added over a 1 h time period. The dichloromethane was slowly evaporated from the bright orange solution by leading a stream of nitrogen over the reaction mixture. During that procedure an orange precipitate
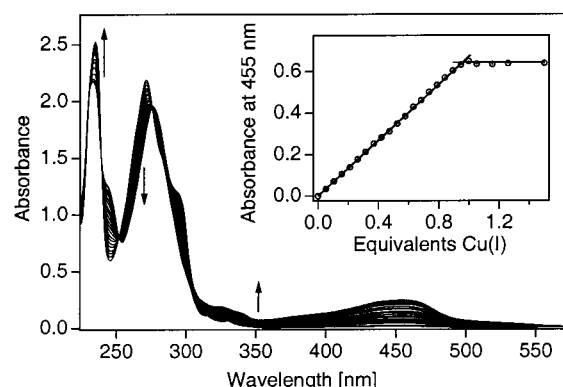
Figure 2. Spectrophotometric titration of **2** with [Cu(CH$_3$CN)$_4$](BF$_4$). The inset shows the absorbance at 455 nm as a function of the Cu(I):**2** ratio (see Experimental Section for details).

formed, which was then collected through vacuum filtration and rinsed thoroughly with acetonitrile and dichloromethane.

Yield: 302 mg (0.42 mmol, 85%) Anal. Calcd for (C$_{38}H_{42}N_4$)-Cu(BF$_4$): C, 64.73; H, 6.00; N, 7.95. Found: C, 64.03; H, 6.11; N, 7.89. ^1H NMR (DMSO-d_6, 400 MHz) δ 8.80−8.60 (2H, m), 8.20−8.0 (2H, bm), 7.95−7.82 (2H, bm), 2.95 (2H, bs), 2.37 (2H, s), 1.1 (2H, bs), 0.45 (4H, bs), 0.20 (4H, bs).

Results and Discussion

Synthesis of Ligands and Coordination Complexes. The synthesis of both bridging ligands was performed using procedures similar to published ones for alkyl-substituted 2,2′-bipyridines and 2,2′:6′,2″-terpyridines (Figure 1).[13] However, the water molecules strongly bound to the diimine functionality of 2,9-dimethyl-1,10-phenanthroline made it necessary to use an excess of base in order to generate the carbanion. The ligands were fully characterized with ^1H NMR, ^{13}C NMR, high-resolution MS, and elemental analysis. The subsequent coordination reaction of **1** with [Cu(CH$_3$-CN)$_4$](BF$_4$) produced a dimeric compound [Cu$_2$(**1**)$_2$](BF$_4$)$_2$, commonly found using similar bis-neocuroine bridging ligands.[8] The dimeric nature of the compound was unambiguously confirmed through the observation of a 0.5 mass unit difference between the isotope peaks of the ESI mass spectrum.

On the other hand, the use of the much less rigid ligand **2** under comparable reaction conditions led to the formation of a polymeric copper compound [**2**(Cu(**2**))$_n$](BF$_4$)$_n$. A spectrophotometric titration of this polymerization reaction shown in Figure 2, exhibited a new absorption band at 450 nm which, for [Cu(dmp)$_2$](PF$_6$), has been attributed to a metal to ligand charge-transfer transition (MLCT).[14] The titration also established the overall 1:1 stoichiometry between the ligand and the copper centers. Moreover, the presence of sharply defined isosbestic points is consistent with a well-defined equilibrium process.

(13) (a) Mürner, H.; von Zelewsky, A.; Stoeckli-Evans, H. *Inorg. Chem.* **1996**, *35*, 3931−3935. (b) Hayoz, P.; Von Zelewsky, A. *Tetrahedron Lett.* **1992**, *33*, 5165−5168.
(14) (a) Blasse, G.; McMillan, D. R. *Chem. Phys. Lett.* **1978**, *70*, 1. (b) Blaskie, M. W.; McMillan, D. R. *Inorg. Chem.* **1980**, *19*, 3519. (c) Igo, D.; Elder, R.; Heineman, W. *J. Electroanal. Chem.* **1991**, *314*, 45−47
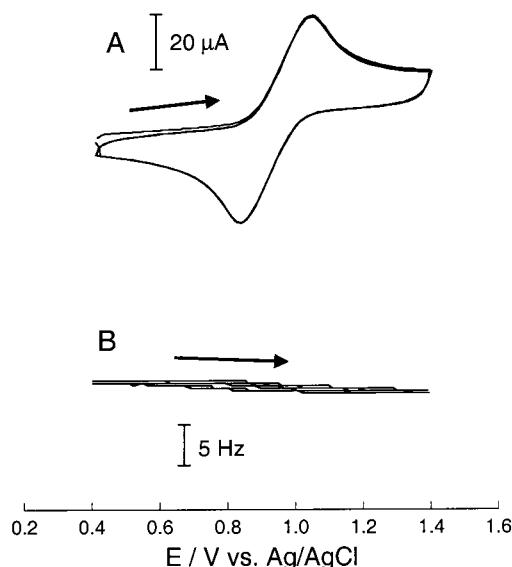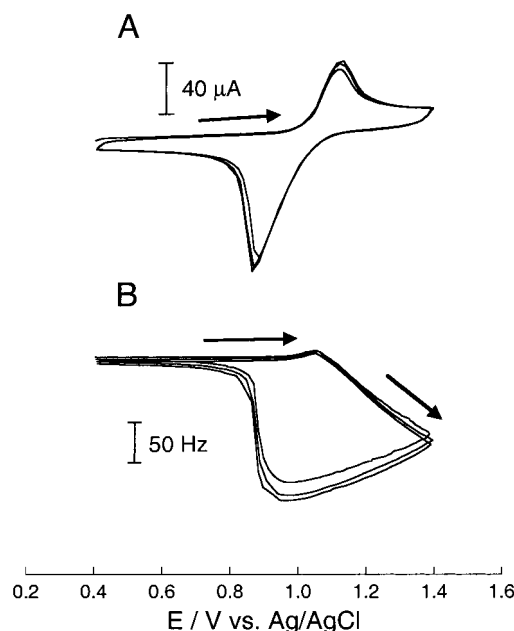
Figure 3. (A) Current (CV) and (B) frequency responses as a function of applied potential at 50 mV s^{-1} for a Pt EQCM electrode in contact with a 0.10 M TBAP/CH$_2$Cl$_2$ solution containing 0.2 mM of [Cu(dmp)$_2$]$^+$.

The polymer was characterized through ^{1}H NMR spectroscopy, elemental analysis, and electrospray mass spectrometry. Attempts to determine the molecular weight through viscometry failed due to the low solubility of the polymer in commonly used solvents.

Electrochemical Studies. The redox behavior of these materials was characterized using cyclic voltammetry (CV) as well as the EQCM technique. Initial studies were carried out using [Cu(dmp)$_2$]$^+$ as a model complex which served as the basis for comparison for studies of the dimeric and polymeric materials. Figure 3 shows the current (cyclic voltammogram; A) and frequency changes (B) as a function of applied potential between +0.40 and +1.40 V vs Ag/AgCl for [Cu(dmp)$_2$]$^+$ in a 0.10 M TBAP/CH$_2$Cl$_2$ solution. The complex exhibits a single redox wave with a formal potential of +0.95 V, attributed to a Cu(I/II) process, which is in concert with previously found potentials for phenanthroline derived Cu complexes.[15] In the above-mentioned EQCM experiment (Figure 3B), the virtually constant value of the frequency implies that the [Cu(dmp)$_2$]$^+$ is not depositing on the surface upon oxidation or reduction. The voltammetric wave shapes for oxidation and reduction also suggest that it is a diffusion controlled process. In addition, the peak current was proportional to the square root of the sweep rate, $v^{1/2}$, as would be anticipated for a diffusion controlled process.

For the dimeric compound [Cu$_2$(**1**)$_2$]$^{2+}$, Figure 4 shows the cyclic voltammogram (A) and the concurrent frequency changes (B) as a function of applied potential between +0.40 and +1.40 V. As in the previous case, there is a wave with a formal potential of +1.00 V which is, again, ascribed to a Cu(I/II) process. The shape of the anodic wave is typical of a diffusion controlled process, and the peak current is proportional to $v^{1/2}$, as would be anticipated. On the other hand, the shape of the reductive wave is much sharper and
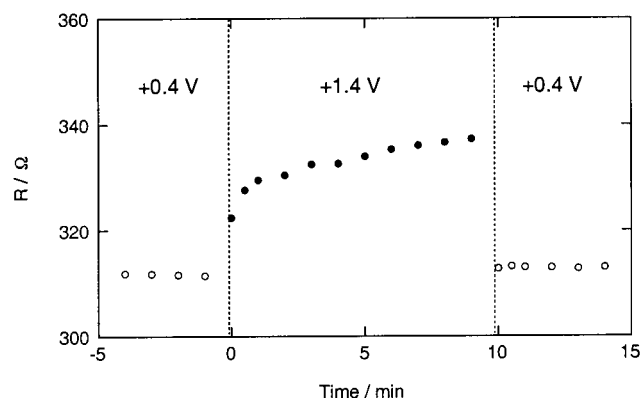
(15) Miller, M.; Karpishin, T. *Inorg. Chem.* **1999**, *38*, 5246−5249.

Figure 4. (A) Current (CV) and (B) frequency responses as a function of applied potential at 50 mV s^{-1} for a Pt EQCM electrode in contact with a 0.10 M TBAP/CH$_2$Cl$_2$ solution containing 0.1 mM (0.2 mM metal site) of [Cu$_2$(**1**)$_2$]$^{2+}$.

"stripping-like", suggesting that the complex adsorbs/precipitates upon oxidation and desorbs/strips upon reduction. The adsorption could also be confirmed by the continuous decrease in frequency upon oxidation. The decrease in frequency with each subsequent cycle indicates the build up of a film on the electrode surface, which is rapidly stripped off upon reduction. The fact that even on the first anodic sweep there was a small increase in frequency (ca. 5 Hz at +1.05 V) would imply that a film is already present on the electrode surface and that cations are being expelled from the surface in order to maintain electrical neutrality. This could be due to the expulsion of either Cu^{2+} from dissociated complex or tetra-*n*-butyl cations. In the latter case, this would necessarily imply that the film present on the surface contains supporting electrolyte as ion pairs.

To study changes in film morphology upon deposition and redissolution, admittance measurements of the quartz crystal resonator, on the basis of its electrical equivalent circuit, particularly the resistance parameter, were conducted. Figure 5 shows the changes in the resistance parameter for the equivalent circuit of the resonator versus time at applied potentials of +0.40 and +1.40 V, where the charges of the complex are +1 and +2, respectively. For [Cu$_2$(**1**)$_2$]$^{2+}$ (Figure 5), there was an increase in resistance at +1.40 V which we attributed to an increase in film thickness, since it continually increased with time. Moreover, the resistance dropped back to the original value when the potential was stepped back to +0.40 V. These results were reproducible for multiple steps. This finding is in accord with the data from the EQCM experiment, since both demonstrate the generation of a film on the surface upon oxidation of the complex and stripping upon reduction.

Figure 6 shows the cyclic voltammogram (A) and the frequency changes (B) as a function of applied potential for
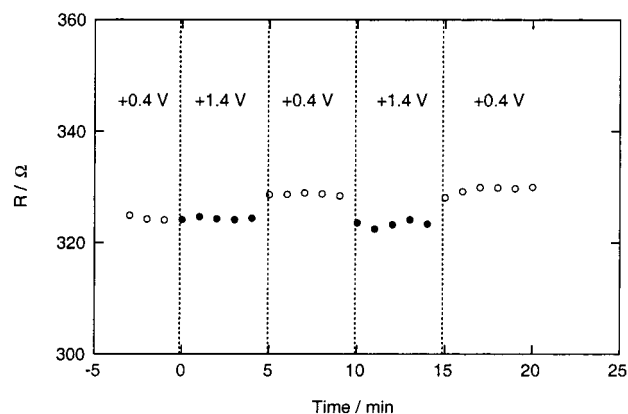
Figure 5. Changes in resistance parameter as a function of applied potential and time for the equivalent circuit of the resonator at applied potentials of +0.40 and +1.40 V vs Ag/AgCl in a 0.10 M TBAP/CH$_2$Cl$_2$ solution containing 0.1 mM (0.2 mM metal site) of [Cu$_2$(**1**)$_2$]$^{2+}$.
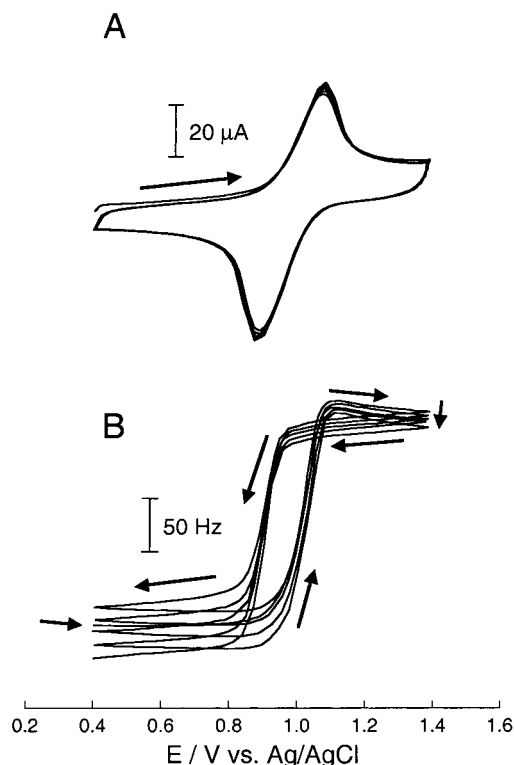
Figure 6. (A) Current (CV) and (B) frequency responses as a function of applied potential at 50 mV s^{-1} for a Pt EQCM electrode in contact with a 0.10 M TBAP/CH$_2$Cl$_2$ solution containing 0.2 mM (metal site) of [**2**(Cu(**2**))$_n$]$^{n+}$.

[**2**(Cu(**2**))$_n$]$^{n+}$. As in the case of [Cu(dmp)$_2$]$^+$ and [Cu$_2$(**1**)$_2$]$^{2+}$, the cyclic voltammogram (Figure 6A) exhibits a wave with a formal potential of +1.00 V, ascribed to a Cu(I/II) redox process. However, it is also evident that, contrary to the behavior of [Cu$_2$(**1**)$_2$]$^{2+}$, the cathodic sweep did not have a "stripping-like" shape. Also contrary to the behavior of [Cu$_2$(**1**)$_2$]$^{2+}$, the frequency (Figure 6B) decreased during the reduction process (and increased in the oxidative sweep). Although somewhat speculative in our part, we believe that there could be, as discussed earlier for analogous complexes, a change in the coordination geometry from the original tetrahedral structure to a distorted octahedral or trigonal bipyramidal geometry. However, additional ligands would


Figure 7. Changes in resistance parameter as a function of applied potential and time for the equivalent circuit of the resonator at applied potentials of +0.40 and +1.40 V vs Ag/AgCl in a 0.10 M TBAP/CH$_2$Cl$_2$ solution containing 0.2 mM (metal site) of the [**2**(Cu(**2**))$_n$]$^{n+}$.

be required to satisfy the electronic requirements of Cu(II) but neither the solvent (CH$_2$Cl$_2$) nor the supporting electrolyte (TBAP) will be effectual for this purpose. To understand the nature of the electrode processes, closer inspection of the changes in the voltammogram and the EQCM response is necessary. First of all, both anodic and cathodic waves are observed, suggesting a simple redox process. It is also apparent that the peak currents for the oxidation and the reduction processes are similar, indicating that the reduced and oxidized species are chemically stable within the cyclic voltammetric time scale. These observations would suggest that if there is partial dissociation (due to the structural changes induced by the redox reaction), there is rapid recapture upon reduction. This assertion is also consistent with the EQCM measurements.

A plausible explanation of the observed results is to assume structural changes in the polymer layer covering the electrode during the Cu(I/II) oxidation and the subsequent reversal of this processes during the reduction step. The fact that the peak currents are growing and the resonance frequency of the quartz crystal is decreasing upon repetitive scanning can be attributed to electrodeposition of the polymer.

As in the previous cases, admittance measurements of the quartz crystal resonator were carried out and are presented in Figure 7. As can be observed, the resistance parameter remained constant upon oxidation but increased upon reduction, demonstrating that there is an increase in film thickness and/or changes in the properties of the film upon reduction. This result is consistent with EQCM data which showed that reduction gave rise to a decrease in frequency which could arise from an increase in the amount of deposited material or to changes in the properties of the film. However, upon comparing the magnitude of the changes in the resistance parameters with the frequency variations in the EQCM experiment, we conclude that both the amount of deposited material and the film properties are changing.

To confirm the mechanism of a redox induced reversible structural transformation in [**2**(Cu(**2**))$_n$]$^{n+}$, EQCM experiments were carried out in the presence of 2,2'-bipyridine in solution. The intent was to have an electrolyte solution
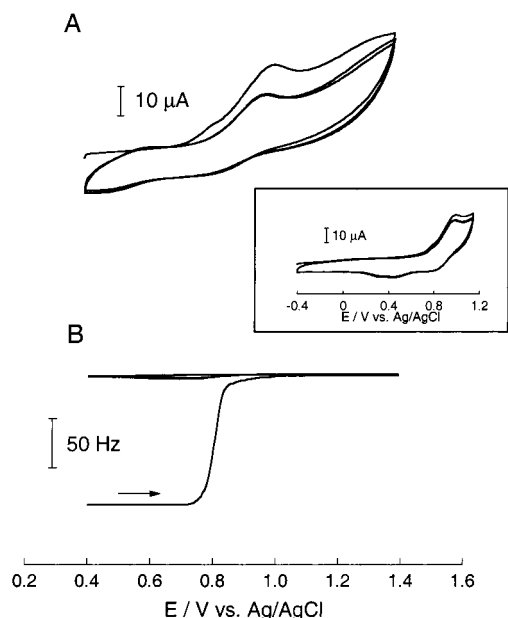
Figure 8. (A) Current (CV) and (B) frequency responses as a function of applied potential at 50 mV s^{-1} for a Pt EQCM electrode in contact with a 0.10 M TBAP/CH$_2$Cl$_2$ solution containing 0.2 mM (metal site) of [**2**(Cu(**2**))$_n$]$^{n+}$ and 0.2 mM 2,2′-bipyridine. Inset is the CV scanned to −0.40 V vs Ag/AgCl.

containing a ligand capable of displacing the equilibrium toward dissociation and concomitant formation of soluble oligomeric fragments. The frequency increase during the initial scan from +0.40 V to +1.40 V was comparable to that obtained in the absence of 2,2′-bipyridine. (Figure 8). However, the frequency response upon scan reversal showed that this increase, earlier assigned to (reversible) structural changes in the polymer film covering the electrode, is no longer reversible under these conditions; i.e., in the presence of 2,2′-bipyridine in solution. This result is corroborated by the diminution of the cathodic peak current in the presence of 2,2′-bipyridine. This confirms fragmentation of the polymer upon oxidation through a subsequent coordination reaction of the generated Cu(II) species by the 2,2′-bipyridine

Table 1. Diffusion Coefficients of Cu Complexes upon Cu$^{I/II}$ Oxidation Determined via the Rotating Disk Electrode Technique in a 0.10 M TBAP/CH$_2$Cl$_2$ Solution
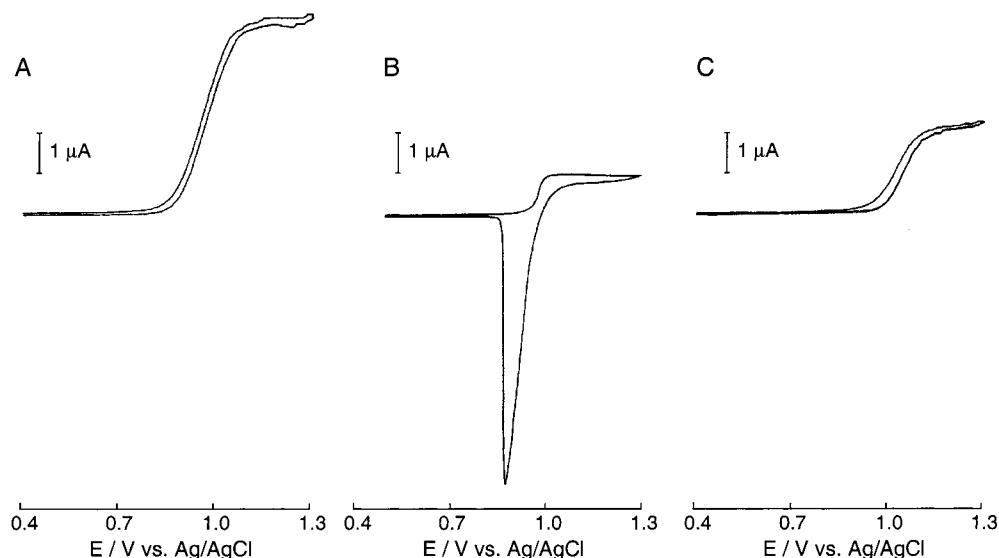
	[Cu(dmp)$_2$]$^+$	[Cu$_2$(**1**)$_2$]$^{2+}$	[**2**(Cu(**2**))$_n$]$^{n+}$
diffusion coefficient (cm^2/s)	6.3 × 10^{-6}	7.4 × 10^{-7}	1.5 × 10^{-6}
radius (Å)	9	77[a]	38

[a] Unphysically large due to adsorption.

present in solution. Moreover, the apperance of a new redox wave at about +0.40 V (typical of 2,2′-bipyridine complexes) is also consistent with and lends further confirmation to our assertions.

Diffusion Coefficient Determination

The diffusion coefficients of the Cu complexes were determined by the rotating disk electrode technique (RDE). Figure 9 shows typical voltammograms of the Cu(I/II) redox process at a scan rate of 20 mV s^{-1} for (A) [Cu(dmp)$_2$](BF$_4$), (B) [Cu$_2$(**1**)$_2$](BF$_4$)$_2$, and (C) [**2**(Cu(**2**))$_n$](BF$_4$)$_n$ in 0.10 M TBAP/CH$_2$Cl$_2$ solutions containing 0.2 mM (metal center) of each complex. From the voltammograms at various rates of rotation (ω), the diffusion coefficients were determined using the linear portions of the Levich plots (I_{lim} vs $\omega^{1/2}$), and the calculated values are presented in Table 1. As anticipated, the diffusion coefficient of [Cu(dmp)$_2$]$^+$ is larger than that of the polymeric [**2**(Cu(**2**))$_n$]$^{n+}$, likely due to the smaller size of the former. However, it is also clear from Table 1 that the diffusion coefficient of [Cu$_2$(**1**)$_2$]$^{2+}$ is smaller than those of [Cu(dmp)$_2$]$^+$ and [**2**(Cu(**2**))$_n$]$^{n+}$. We believe that this arises, at least in part, from the deposited [Cu$_2$(**1**)$_2$]$^{2+}$ present on the electrode, which blocks the diffusion of the species in solution. As can be seen in Figure 9B, the voltammogram of [Cu$_2$(**1**)$_2$]$^{2+}$ shows a sharp peak upon reduction, indicating that there is a deposited film of [Cu$_2$-(**1**)$_2$]$^{2+}$ on the electrode and that the film is rapidly stripped upon reduction (recall earlier discussion). Thus, the diffusion coefficient for [Cu$_2$(**1**)$_2$]$^{2+}$ is not considered reliable. Although [**2**(Cu(**2**))$_n$]$^{n+}$ also deposits onto the electrode, as
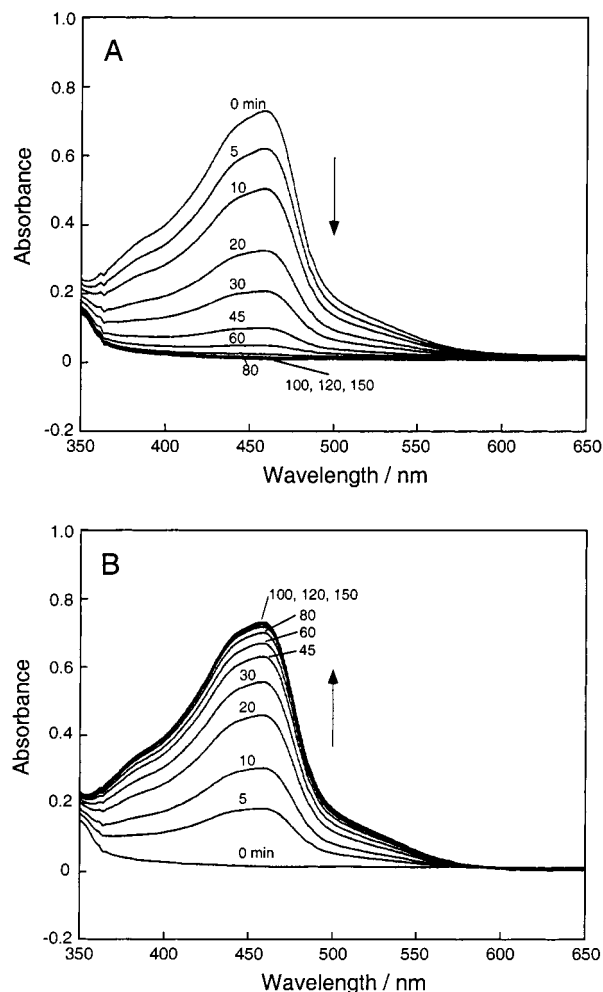

Figure 9. Cyclic voltammograms of RDE (Pt) at 200 rpm in a 0.10 M TBAP/CH$_2$Cl$_2$ solution containing 0.2 mM (metal site) of (A) [Cu(dmp)$_2$]$^+$, (B) [Cu$_2$(**1**)$_2$]$^{2+}$, and (C) [**2**(Cu(**2**))$_n$]$^{n+}$. Potential scan rates are at 5 mV s^{-1}.

mentioned in the EQCM section, the deposition takes place upon reduction, contrary to $[Cu_2(1)_2]^{2+}$. In addition, to mitigate the effects of adsorbed material in the determination of the diffusion coefficients, the electrode was polished after each measurement at each rate of rotation. Further insight could be gained by combining the measured values of the diffusion coefficients and the Stokes−Einstein formulation for diffusion.

$$D = kT/6\pi R\eta \qquad (1)$$

where D is the diffusion coefficient, k is the Boltzmann constant, R is the radius of a spherical particle, η is the viscosity of the solution, and the remaining symbols have their usual meaning.[15] Using this equation and assuming that these species are spherical, their radii were calculated from the experimentally measured diffusion coefficient and the values are presented in Table 1. It is worth noting that the value calculated for $[Cu(dmp)_2]^+$ is in excellent agreement with its known radius determined through X-ray crystallography.[16] For $[2(Cu(2))_n]^{n+}$ the calculated value of the radius was about 4 times that of $[Cu(dmp)_2]^+$, which is about the length of a $[2(Cu(2))_3]^{3+}$ chain. Using the density of the copper polymer (1.15 g/mL), one could also argue that a sphere with a radius of 38 Å filled with $[2(Cu(2))_n](BF_4)_n$ would give rise to a degree of polymerization around 225. However, due to solvent inclusion and imperfect spherical packing of the polymer, the chain length is most probably shorter.

Spectroelectrochemical Studies. Spectroelectrochemical studies were used to further investigate the processes occurring during the reduction/oxidation reaction at the copper centers. Figure 10A shows the changes in absorption as a function of time for different potentials applied to a solution of $[2(Cu(2))_n]^{n+}$ in 0.10 M TBAP/CH$_2$Cl$_2$. The potential was initially stepped from +0.40 to +1.40 V vs Ag/AgCl. Following this potential step, the peak at 455 nm diminished in amplitude (absorbance) over a period of 150 min. It is worth mentioning that in analogous studies of discrete copper complexes the electrolysis time is of the order of 30 min. An increase in time of the electrolysis is not unanticipated given the relative size of the complexes, particularly $[2(Cu(2))_n]^{n+}$, which would, in turn, affect the diffusion coefficient and, hence, transport. The peak at 455 nm is attributed to a MLCT transition due to the copper(I)/2,9-alkyl-1,10-phenanthroline coordination.[14] The disappearance of this absorption band indicates that the complex is completely oxidized, but one cannot, solely on the basis of these results, unambiguously distinguish between dissociated and polymerically bound Cu(II). Figure 10B shows the spectral changes of the same sample after the potential was stepped back to +0.40 V. The increase in absorption up to the original levels suggests that $[2(Cu(2))_n]^{n+}$ is re-forming upon reduction, which indicates that the process of binding/unbinding in this system is reversible, if kinetically slow.

(16) Einstein, A. In *Investigations on the Theory of the Brownian Movement*; Fürth, R., Ed.; Methuen & Co. Ltd.: London, 1926; Section I.

(17) Dessy, G.; Fares, V. *Cryst. Struct. Commun.* **1979**, *8*, 507−510.
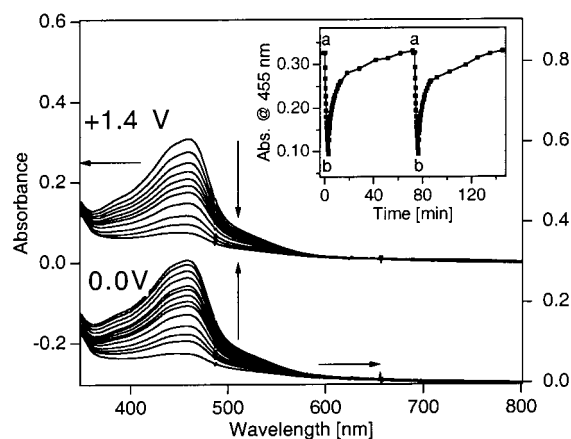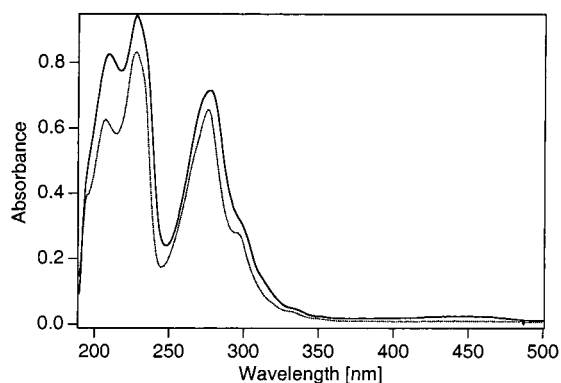

Figure 10. Spectral changes in the visible region upon (A) oxidation at +1.40 V and (B) reduction at +0.40 V vs Ag/AgCl of 0.1 mM (metal center) $[2(Cu(2))_n]^{n+}$ in a 0.10 M TBAP/CH$_2$Cl$_2$ solution. The working electrode is a Pt mesh.

The fact, that the electrolysis time for the reduction is comparable to that of the preceding oxidation indicates that the polymer in its oxidized state is not fragmented. To understand the mechanism of dissociation severing these chains, experiments were performed in an aqueous electrolyte. The presence of water makes the disruption of the chains (following oxidation) more likely than in the weakly coordinating CH$_2$Cl$_2$ solvent. However, due to the insolubility of the polymer in aqueous electrolyte solutions, it was necessary to observe the oxidation process starting from a film cast on an ITO (indium−tin oxide) electrode. Figure 11 depicts the spectral changes as a function of applied potential of this coated electrode in 0.1 M LiClO$_4$ in 1:1 ethanol:water. The top panel shows the spectral changes following a potential step to +1.40 V, whereas the bottom panel shows the spectral changes after stepping the potential back to 0.0 V. The inset shows the time evolution of the absorbance at 455 nm. As can be ascertained from the figure, oxidation at +1.40 V (a in the inset) results in a rapid decrease in the absorbance, reaching a minimum in about 5 min. Stepping the potential back to 0.0 V (b in the inset) results in the recovery of the absorbance at 455 nm, but this is a significantly slower process, taking approximately 75

Figure 11. Spectral changes in the visible region upon oxidation and reduction of the copper centers of a $[2(Cu(2))_n](BF_4)_n$ film on a ITO electrode in a 0.1 M LiClO$_4$ ethanol:water (1:1) electrolyte solution. The inset presents the time dependence of the absorbance at 455 nm. (a, 0.00 V → 1.40 V; b, 1.40 V → 0.00 V).

Figure 12. (−) Spectrum of the electrolyte solution after complete oxidation of a $[2(Cu(2))_n](BF_4)_n$ film on a ITO electrode in a 0.1 M LiClO$_4$ ethanol:water (1:1) electrolyte.solution. (--) 10 mM solution of Cu(ClO$_4$)$_2$ and 2,9-dimethyl-1,10-phenanthroline in 0.1 M LiClO$_4$ ethanol:water (1:1).

min. However, the reversibility of the process is clearly established. The difference in the rates of dissociation (stripping or dissolution) vs regeneration (redeposition as a Cu(I) film) is not an unexpected result given that the former would be anticipated to be much faster than the latter, as was indeed observed.

The nature of the electrogenerated Cu(II) species in solution was further investigated by obtaining the UV spectrum of a solution after complete oxidation of a film (resulting in the generation of ostensibly $[Cu(2)(H_2O)_n]^{2+}$) deposited as above. Figure 12 (solid line) presents the spectrum (in 0.1 M LiClO$_4$ in 1:1 ethanol:water) of a film after complete oxidation at +1.40 V. Also presented in Figure 12 (dotted line) is the spectrum of a 10 μM solution of Cu(ClO$_4$)$_2$ and 2,9-dimethyl-1,10-phenanthroline. The similarity of the spectra is immediately apparent and serves to further support our assertions concerning the coordination changes following oxidation and reduction of the copper centers.

Conclusions

The synthesis and characterization of copper complexes of the phenanthroline-based bridging ligands, 9-methyl-2-(2-{4-[2-(9-methyl-1,10-phenanthrolin-2-yl)ethyl]phenyl}-ethyl)-1,10-phenanthroline, **1**, and 1,12-bis(9-methyl-1,10-phenanthroline -2-yl)dodecane, **2**, are presented. Whereas in the first case a discrete dimeric complex $[Cu_2(1)_2]^{2+}$ was formed, in the latter a coordination polymer $[2(Cu(2))_n]^{n+}$ resulted. Both of these materials have been characterized by CV, EQCM, and UV−vis spectroscopy, and the results compared to those of the monomeric $[Cu(dmp)_2]^+$ (dmp is 2,9-dimethyl-1,10-phenanthroline) species. Oxidation of the dimeric species results in its precipitation, and subsequent reduction leads to the stripping of the deposited layer as ascertained from CV and EQCM measurements. The electrooxidation of the copper centers in the coordination polymer results in changes in the coordination which are fully reversible upon reduction. The dissociation/regeneration of the coordination polymer as a function of the redox state of the copper centers has been characterized by CV, EQCM, and UV−vis spectroelectrochemistry.

Although the dissociation/regeneration cycles are slow, these types of materials could find numerous applications in areas such as electroresponsive reversible membranes and controlled transport materials. These areas are currently being pursued.